

SAR and in vivo evaluation of 4-aryl-2-aminoalkylpyrimidines as potent and selective Janus kinase 2 (JAK2) inhibitors

Timothy Forsyth, Patrick C. Kearney, Byung Gyu Kim*, Henry W. B. Johnson*, Naing Aay, Arlyn Arcalas, David S. Brown, Vicky Chan, Jeff Chen, Hongwang Du, Sergey Epshteyn, Adam A. Galan, Tai P. Huynh, Mohamed A. Ibrahim, Brian Kane, Elena S. Koltun, Grace Mann, Lisa E. Meyr, Matthew S. Lee, Gary L. Lewis, Robin T. Noguchi, Michael Pack, Brian H. Ridgway, Xian Shi, Craig S. Takeuchi, Peiwen Zu, James W. Leahy, John M. Nuss, Ron Aoyama, Stefan Engst, Steven B. Gendreau, Robert Kassees, Jia Li, Shwu-Hwa Lin, Jean-Francois Martini, Thomas Stout, Philip Tong, John Woolfrey, Wentao Zhang, Peiwen Yu

Exelixis, Department of Drug Discovery, 169 Harbor Way, South San Francisco, CA 94083, USA

ARTICLE INFO

Article history:

Received 29 July 2012

Revised 26 September 2012

Accepted 1 October 2012

Available online 16 October 2012

Keywords:

JAK1

JAK2

JAK3

4-Aryl-2-aminoalkylpyrimidine

ABSTRACT

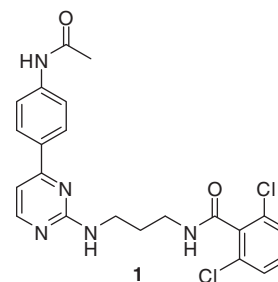
We report the discovery of a series of 4-aryl-2-aminoalkylpyrimidine derivatives as potent and selective JAK2 inhibitors. High throughput screening of our in-house compound library led to the identification of hit **1**, from which optimization resulted in the discovery of highly potent and selective JAK2 inhibitors. Advanced lead **10d** demonstrated a significant dose-dependent pharmacodynamic and antitumor effect in a mouse xenograft model. Based upon the desirable profile of **10d** (XL019) it was advanced into clinical trials.

© 2012 Elsevier Ltd. All rights reserved.

Janus kinase 2 nonreceptor tyrosine kinase, a member of the JAK family of kinases (JAK1, JAK2, JAK3, and TYK2), has garnered a tremendous amount of attention in recent years since the discovery of a somatic mutation of the gene encoding JAK2 (JAK2^{V617F}).^{1–5} The V617F mutation occurs in the auto-inhibitory JH2 domain and is thought to disrupt its negative regulatory function. This leads to constitutive activation of JAK2, downstream signal transducer and activators of transcription (STAT), and activation of gene transcription. A frequent point mutation of JAK2 was identified in myeloproliferative disorders (MPDs) including polycythemia vera (PV), essential thrombocythemia (ET), and primary myelofibrosis (PMF). Recent approval of ruxolitinib⁶ (JAK1/2 inhibitor), developed by Incyte and Novartis, has clinically validated JAK2 for the treatment of MPDs. Not surprisingly, several JAK2 selective inhibitors have been developed and are currently being tested in clinical trials.^{7–14} Herein, we report our efforts in the identification and SAR exploration of potent and selective JAK2 inhibitors.

High Throughput Screening (HTS) of our in-house compound library revealed hit **1** that was considered a good starting point for

our investigation (Fig. 1). Compound **1** displayed potent inhibitory activity against JAK2 with >50-fold selectivity over JAK3 along with no activity below 5000 nM against a broad in-house panel of kinases. In addition, **1** possessed reasonable in vitro stability (62% remained after exposure of **1** to mouse liver microsomes for



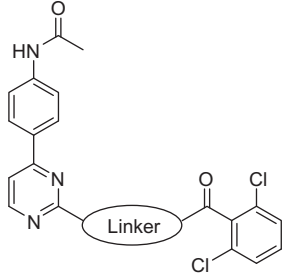
JAK2 : 104 nM
JAK3 : >5000 nM

Figure 1. HTS hit **1**.

* Corresponding authors.

E-mail addresses: byunggyu72kim@gmail.com (B.G. Kim), hjohnson@onyx.com (H.W.B. Johnson).

Table 1
Optimization of the linker



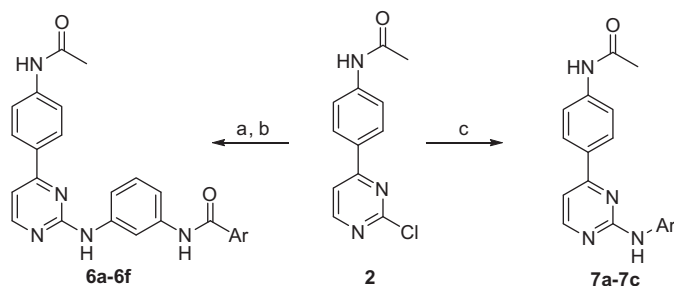
ID	Linker	JAK2 (nM) ^a	JAK3 (nM) ^a	pStat1 (nM) ^a	pStat3 (nM) ^a
1		104	>5,000	8,138	n.d.
3		>980	>980	>30,000	n.d.
4		5000	5000	>30,000	n.d.
5		12.6	>980	763	505
6		129.9	>980	>30,000	n.d.

n.d. = not determined.

^a Values reported are the average of at least two independent dose-response curves.¹⁷

30 min) and acceptable drug-like properties ($c\text{Log}P = 3.1$, PSA 96 Å, MW = 458). However, the poor cellular activity ($\text{IC}_{50} = 8138 \text{ nM}$ (pStat1 in HEL92.1.7)) and solubility ($K_{\text{sol}} = 6.5 \mu\text{M}$), along with moderate biochemical potency ($\text{IC}_{50} = 104 \text{ nM}$) of **1** required improvement.

Rigidifying the linker between the aminopyrimidine and 2,6-dichlorophenylamide was considered a viable method to potentially improve the potency. We initiated our SAR studies by constructing analogues that replaced the 1,3-propyldiamine with a different functional group (Table 1). Both 1,3-cyclohexyldiamine **3** and azetidin-3-ylmethanamine **4** led to complete loss of JAK2 biochemical activity. Gratifyingly, 1,3-phenylenediamine analogue **5** improved not only JAK2 biochemical activity but also the cellular activity. Analogue **6** containing the 2,6-diaminopyridine displayed 10-fold weaker JAK2 potency compared to **5**. The analogues in Table 1 were prepared by Suzuki coupling reaction¹⁵ of 2,4-dichloropyrimidine

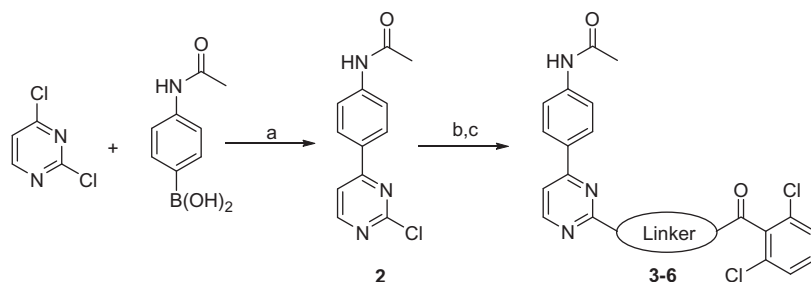


Scheme 2. ¹⁷Reagents and conditions: (a) Et_3N , *N*-Boc-amino-3-aniline, 1-butanol, 180 °C; HCl, MeOH; (b) DIEA, THF, arylbenzoyl chloride, 70 °C or DIEA, DMF, HATU, arylbenzoic acid; (c) ArNH_2 , 1-butanol, 180 °C.

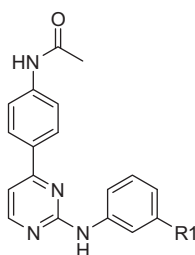
with 4-acetylphenylboronic acid to afford **2** (Scheme 1). Nucleophilic substitution of **2** with alkylamine or arylamine followed by an amide coupling with 2,6-dichlorobenzoyl chloride provided compounds **3–6**.

Having a derivative in hand with improved potency we next turned our attention to modification of the aryl amide. Several analogues were prepared with the 1,3-diaminophenyl linker using the route shown in Scheme 2. In order to improve the solubility of this series, modification of the lipophilic aryl amide was considered critical (Table 2). Deletion of chloride substitution at the *ortho* position (**6a** and **6b**) retained JAK2 biochemical potency with similar selectivity against JAK3. Interestingly, simple aniline **6c** retained both biochemical activity and cellular activity. Removal of the aryl amide also provided a significant increase in solubility ($K_{\text{sol}} = 233.8 \mu\text{M}$) compared to the aryl amide analogues in the series. Encouraged by this result, additional analogues were synthesized lacking the aryl amide. Meta piperidine substitution (**7a**) displayed slightly improved biochemical and cellular potency compared to **6c**. The 3-morpholine analogue **7b** provided a modest improvement in both biochemical and cellular potency compared to **7a**. In addition, the 4-morpholine analogue **7c** retained JAK2 potency with similar selectivity against JAK3. The analogues **6a–6c** were prepared by nucleophilic substitution of **2** with *N*-Boc-amino-3-aniline, followed by Boc deprotection and amide coupling with either arylbenzoyl chloride or arylbenzoic acid (Scheme 2). The analogues **7a–7c** were synthesized by a nucleophilic substitution reaction of **2** with the appropriate aniline.

Subsequent modification involved the scaffold aminopyrimidine core. Moving the nitrogen from C-3 to C-5 (**9a**) led to the complete loss of JAK2 activity, presumably due to a weaker interaction with the hinge region and/or a steric repulsion of the C-3 hydrogen and the hydrogen *ortho* on the morpholinoaniline moiety; a modification which would force the two rings out of planarity. Fluoride substitution (**9b**) at C-5 maintained biochemical potency but suffered from a significant loss of cellular potency. Analogue **9c** with a methyl at C-5 had a similar potency profile to **7c** but a significantly less desirable



Scheme 1. ¹⁷Reagents and conditions: (a) Et_3N , Pd(dppf) $\text{Cl}_2 \cdot \text{CH}_2\text{Cl}_2$, DME/ H_2O , 90 °C; (b) Linker, 1-butanol, 180 °C; (c) DIEA, THF, 2,6-dichlorobenzoyl chloride, 70 °C. Linker = 1,3-propyldiamine, 1,3-cyclohexyldiamine, azetidin-3-ylmethanamine, 1,3-phenyldiamine, 2,6-diaminopyridine.

Table 2
SAR on the right-hand side


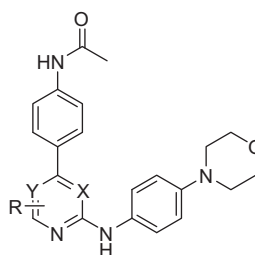
ID	R1	JAK2 (nM) ^a	JAK3 (nM) ^a	pStat1 (nM) ^a	pStat3 (nM) ^a
5		12.6	>980	763	n.d.
6a		6.9	>980	>30,000	n.d.
6b		11.1	>980	>30,000	n.d.
6c	H	12.8	1149.3	1004.3	1971
7a		6.5	>980	956.1	1328
7b		4.2	>980	615	591
7c	4-Morpholine	3.6	>980	974.7	795

n.d. = not determined.

^a Values reported are the average of at least two independent dose-response curves.¹⁷

selectivity profile against JAK3. Analogue **9d** with trifluoromethyl at C-5 demonstrated 10-fold weaker biochemical potency relative to **7c**. Analogue **9e** with 6-methyl was inactive against JAK2; a feature that is not surprising as this substitution would likely disrupt hydrogen bonding with the kinase linker.

The synthesis of analogues in Table 3 started from the appropriately substituted 2,4-dichloropyrimidine or 4,6-dichloropyrimidine, which was subjected to a Suzuki coupling reaction with 4-acetylphenylboronic acid to produce **8** (Scheme 3). Nucleophilic substitution of **8** with 4-morpholinoaniline in 1-butanol at 180 °C afforded compounds **9a–9e**. Despite our effort, modification of the pyrimidine core did not result in an improvement in potency over parent **7c**.

Table 3
SAR on the pyrimidine ring


ID	X	Y	R	JAK2 (nM) ^a	JAK3 (nM) ^a	pStat1 (nM) ^a	pStat3 (nM) ^a
7c	N	CH	H	3.6	>980	974.7	795
9a	CH	N	H	>980	>980	>30,000	n.d.
9b	N	CH	5-F	4.4	>980	6486.7	n.d.
9c	N	CH	5-CH ₃	5.1	104.5	608.9	447
9d	N	CH	5-CF ₃	39.6	>980	2699.9	n.d.
9e	N	CH	6-CH ₃	>980	>980	>30,000	n.d.

n.d. = not determined.

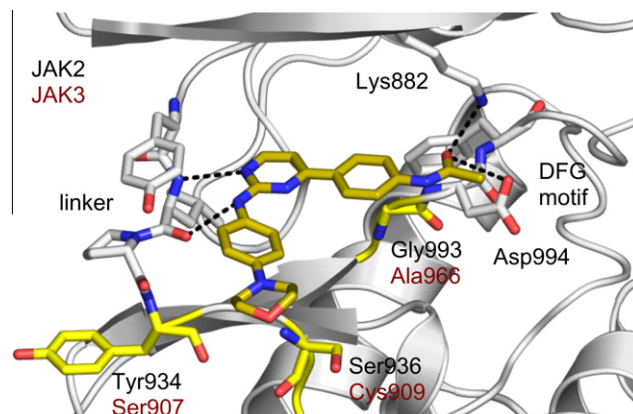
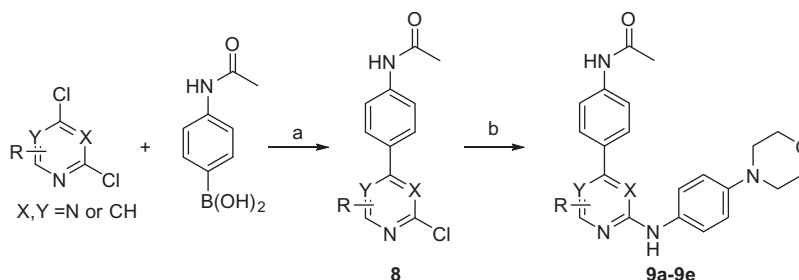
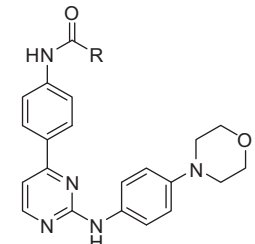
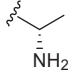
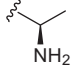
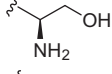
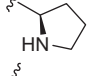
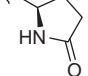
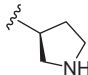
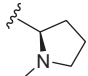
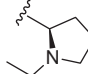
^a Values reported are the average of at least two independent dose-response curves.¹⁷

Figure 2. Cocrystal structure of **7c**/JAK2 solved at 1.9 Å resolution (PDB Code 4BBE). **7c** exhibits an L-shape between the kinase ATP binding pocket. Two hydrogen bonds are formed between the aminopyrimidine ring and the linker region of the kinase. The acetyl oxygen interacts with Asp994 (part of the DFG motif) and Lys882. Residues in the active site of JAK2 that are different in JAK3 are highlighted in yellow. Hydrogen bonding interactions between **7c** and JAK2 <3.3 Å are indicated.



Scheme 3. ¹⁷Reagents and conditions: (a) Et₃N, Pd(dppf) Cl₂·CH₂Cl₂, DME/H₂O, 90 °C; (b) 4-morpholinoaniline, 1-butanol, 180 °C.

Table 4
Optimization of acetimide


ID	R	JAK2 (nM) ^a	JAK3 (nM) ^a	pStat1 (nM) ^a	pStat3 (nM) ^a
7c	Me	3.6	>980	974.7	795
10a		8.7	298.3	1052.5	1510
10b		1.7	306.8	327.7	452
10c		2.7	159.8	621.7	1391
10d		2.2	214.2	386.4	695
10e		0.9	61.7	>30,000	n.d.
10f		5.7	368.1	>30,000	n.d.
10g		5.2	483.8	745.7	1051
10h		9.1	557.3	1431.3	2166

n.d. = not determined.

^a Values reported are the average of at least two independent dose-response curves.¹⁷

To facilitate optimization, an X-ray cocrystal structure of **7c** bound to the ATP binding site of JAK2 was obtained (Fig. 2). Hydrogen bonding interactions of **7c** with JAK2 occurs with both the linker and salt bridge residues Asp994 and Lys882. The morpholino group is solvent exposed and does not appear to make specific interactions with the target, thereby providing an explanation for the wide variety of functionality tolerated in this region. Surpris-

ingly despite the high degree of homology between JAK2 and JAK3, a >250-fold difference in selectivity was observed with **7c**.

Although a rationale for the excellent selectivity of **7c** was not readily apparent, our attention was turned to modifying the amide of **7c**. The cocrystal structure indicated that polar functionality would likely be tolerated and consequently could serve to decrease the lipophilicity of **7c**. Thus, a focused library of amide compounds was prepared from the corresponding aniline and a summary of this data is provided in Table 4. From this study it was observed that analogues containing a heteroatom α or β to the amide were well tolerated. For example, while L-glycine analogue **10a** displayed slightly weaker activity, D-glycine analogue **10b** improved cellular activity threefold compared to **7c**. Both D-serine analogue **10c** and D-proline analogue **10d** showed a similar improvement in cellular activity although the selectivity against JAK3 was modestly eroded. Surprisingly, the D-pyrroglutamic acid (**10f**) and 3-substituted D-pyrrolidine (**10e**) derivatives were completely inactive in the cellular assay although they retained similar biochemical activity. Substitution of nitrogen on the D-proline (**10g–10h**) revealed a modest loss of both biochemical and cellular activity.

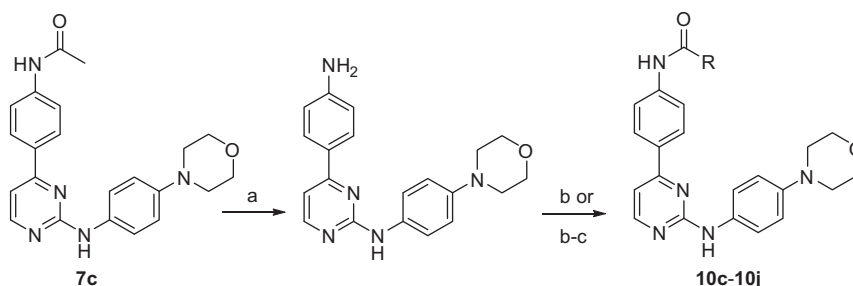
The synthesis of analogues **10a–10h** is shown in Scheme 4. Deacetylation of **7c** in refluxing acid yielded the aniline, which was then coupled with the N-Boc protected appropriate acid in the presence of HATU followed by Boc deprotection to afford analogues **10a–10d** and **10f**. Analogues **10e** and **10g–10h** were synthesized via a HATU coupling reaction of the aniline and appropriate acid.

An X-ray cocrystal structure of **10d** bound to the active site of JAK2 indicated that a similar binding mode is observed for **7c** and **10d**, however the amide of **10d** is rotated to accommodate the larger pyrrolidine ring (Fig. 3).

The desirable in vitro potency of **10d** prompted further investigation in a pharmacodynamic study.¹⁶ Analogue **10d** was administered orally to mice bearing HEL92.1.7 tumors and inhibition of STAT phosphorylation was measured after 4 h. A significant inhibition of downstream markers pSTAT1 and pSTAT3 is observed at 30, 100, and 300 mg/kg resulting in an ED₅₀ of 42 mg/kg (pSTAT1) and 210 mg/kg (pSTAT3) (Table 5).

Further in vivo characterization of advanced acetamide analogues indicated that **10d** had a superior pharmacodynamic profile and thus was evaluated in an efficacy experiment measuring growth inhibition of HEL92.1.7 xenograft tumors in mice (Fig. 4). Derivative **10d** demonstrated 60% and 70% inhibition when dosed orally at 200 mg/kg and 300 mg/kg respectively twice a day for 14 days. Harvested tumors were also subjected to immunohistochemical analysis of microvessel density (CD31), proliferation (Ki67) and apoptosis (TUNEL). Dosing at 300 mg/kg bid provided an 11.3-fold increase in apoptosis relative to vehicle control.

Pharmacokinetic data collected for **10d** in mouse, rat, dog, and monkey are summarized in Table 6. Generally, compound **10d** exhibited good oral absorption, and modest clearance and half life across species.

**Scheme 4.** ¹⁷Reagents and conditions: (a) 6 N HCl, MeOH, reflux; (b) RCO₂H, Et₃N, HATU, DMA; (c) HCl, 1,4-dioxane.

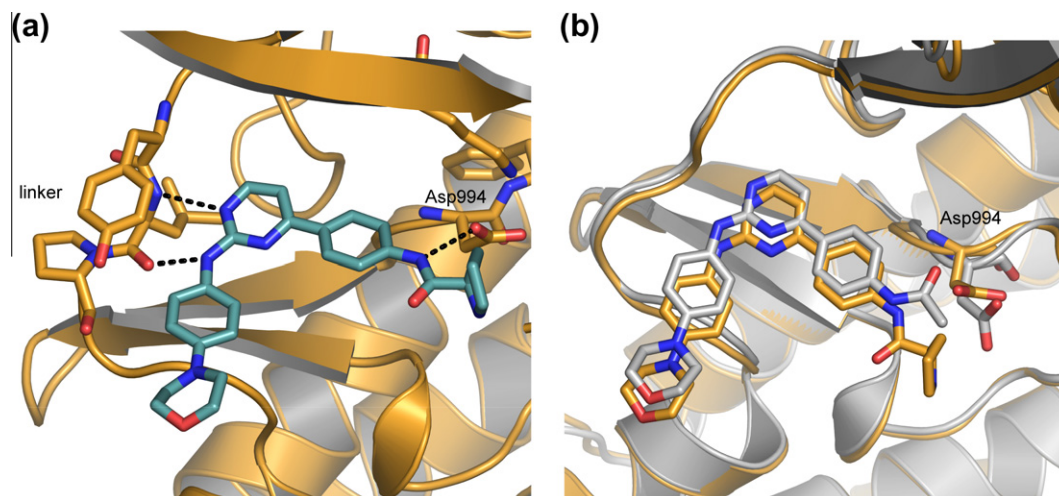


Figure 3. (a) Cocystal structure of **10d**/JAK2 solved at 2.0 Å resolution (PDB Code 4BBF). A similar L-shaped binding mode is observed for **7c** and **10d** within the JAK2 active site. Hydrogen bonding interactions between **10d** and JAK2 <3.1 Å are indicated. (b) Overlay of the cocystal structures of **7c**/JAK2 (grey) and **10d**/JAK2 (orange). The amide of **10d** is rotated to allow a hydrogen bond between the nitrogen and Asp994 of the DFG motif.

Table 5
In vivo pharmacodynamics of **10d**

Dose	Plasma/tumor Concentration (μM) ^a	% Inhibition pSTAT1/pSTAT3	Est. ED ₅₀ pSTAT1/pSTAT3 (mg/kg)	Est. IC ₅₀ pSTAT1/pSTAT3 (μM)
30	0.83 ± 0.45/2.00 ± 1.02	41/9	42/210	1.39/13.0
100	5.35 ± 1.15/240 ± 6.43	72/40		
300	20.23 ± 8.77/62.4 ± 62.38	88/55		

^a Inhibition of STAT phosphorylation was measured 4 h after treating female nude mice ($n = 4$) implanted with HEL92.1.7 xenograft tumors. Plasma/tumor concentration reported as the mean ± SD. Inhibition reported as the mean ($n = 4$) relative to vehicle. **10d** was formulated in water +10 mM HCl.

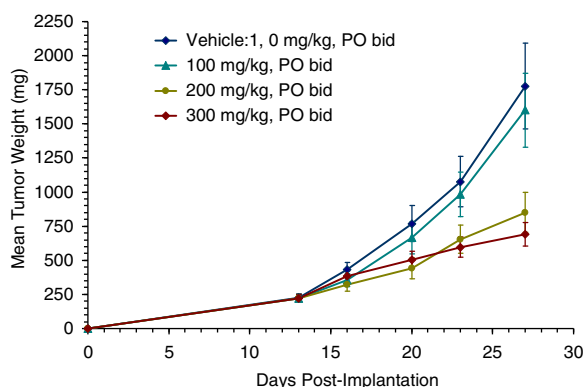


Figure 4. Inhibition of HEL92.1.7 xenograft tumor growth by **10d**. Experiment involved twice daily administration of **10d** to tumor-bearing nude mice over a 14 day period. Data represents mean tumor size ± SE ($n = 10$). Analogue **10d** was formulated in water +10 mM HCl.

Analogue **10d** was also evaluated against a selectivity panel of 118 kinases. Targets for which **10d** exhibited IC₅₀ <1000 nM are displayed in Table 7. Overall **10d** is a highly selective JAK2 inhibitor displaying >50-fold selectivity against all kinases tested including

Table 7
Kinase selectivity profile of **10d**^a

Kinase	IC ₅₀ (nM)	Kinase	IC ₅₀ (nM)	Kinase	IC ₅₀ (nM)
JAK1	134.3	TYK2	348.3	c-KIT	225.8
MLK1	370.0	PDGFRA	546.7	PDGFRB	125.4
FLT3	139.7	FLT4	554.5	KDR	483.6
IKKbeta	375.4	p70S6K	313.8	FLT1	910.5

^a Values reported are the average of at least two independent dose-response curves. All assays were performed at ATP concentrations approximately equal to the K_m values of the respective enzymes.

JAK family members JAK1 and TYK2. Further in vitro evaluation of **10d** revealed that it demonstrated a desirable CYP (1A2, 2C9, 2D6, 3A4 ≥20 μM), hERG (16 μM), and P-glycoprotein inhibition (>20 μM) profile.

In summary, we have discovered a series of potent and selective JAK2 inhibitors. Compound **10d** shows good biochemical and cellular potency against JAK2 with good selectivity against the Janus Kinase family as well as a broad kinase panel. It shows a favorable pharmacokinetic profile and a dose-dependent pharmacodynamic effect in HEL92.1.7 cells. In addition, **10d** induced moderate tumor growth inhibition accompanied by increases in tumor cell apoptosis. Compound **10d** was selected as a clinical candidate and

Table 6
Pharmacokinetic properties of **10d**^{17,18}

Species	Dose (mg/kg)	CL (mL/h/kg)	V _d (L/kg)	T _{1/2} (h) IV / PO	F (%)	C _{max} (μM) IV/PO	AUC/dose ($\mu\text{M h kg/mg}$) IV/PO
Mouse	10	4951.79	5.319	1.13/1.94	54.5	5.24/0.57	0.42/0.21
Rat	5	129.23	0.666	3.12/3.23	53.6	12.95/3.53	15.99/8.54
Dog	3	1397.5	13.4	6.00/5.06	44.8	0.44/0.17	1.47/0.68
Cyno	3	1174.78	6.739	3.28/3.36	68.6	0.64/0.49	1.76/1.20

advanced into human clinical trials where it was evaluated in patients with primary myelofibrosis, post-polycythemia vera, or post-essential thrombocythemia myelofibrosis.¹⁹

Acknowledgments

We greatly appreciate the contributions to the biochemical, cellular, and pharmacokinetic data from members of Exelixis Genome Biochemistry, New Lead Discovery, Molecular and Cellular Pharmacology, Pharmacology, and Compound Repository Groups.

References and notes

- Rane, S. G.; Reddy, E. P. *Oncogene* **2000**, *19*, 5662.
- Levine, R. L.; Wadleigh, M.; Cools, J.; Ebert, B. L.; Wernig, G.; Huntly, B. P.; Boggan, T. J.; Wlodarska, I.; Clark, J. J.; Moore, S.; Adelsperger, J.; Koo, S.; Lee, J. C.; Gabriel, S.; Mercher, T.; D'Andrea, A.; Frohling, S.; Dohner, K.; Marynen, P.; Vandenberghe, P.; Mesa, R. A.; Tefferi, A.; Griffin, J. D.; Eck, M. J.; Sellers, W. R.; Meyerson, M.; Golub, T. R.; Lee, S. J.; Gilliland, D. G. *Cancer Cell* **2005**, *7*, 387.
- Baxter, E. J.; Scott, L. M.; Campbell, P. J.; East, C.; Fourouclas, N.; Swanton, S.; Vassiliou, G. S.; Bench, A. J.; Boyd, E. M.; Curtin, N.; Scott, M. A.; Erber, W. N.; Green, A. R. *Lancet* **2005**, *365*, 1054.
- James, C.; Ugo, V.; Le Couedic, J. P.; Staerk, J.; Delhommeau, F.; Lacout, C.; Garcon, L.; Raslova, H.; Berger, R.; Bennacaur-Griselli, A.; Villeval, J. L.; Constantinescu, S. N.; Casadevall, N.; Vainchenker, W. *Nature* **2005**, *434*, 1144.
- Kralovics, R.; Passamonti, F.; Buser, A. S.; Teo, S.-S.; Tiedt, R.; Passweg, J. R.; Tichelli, A.; Cazzola, M.; Skoda, R. C. *N. Engl. J. Med.* **2005**, *352*, 1779.
- Verstovsek, S.; Mesa, R. A.; Gotlib, J.; Levy, R. S.; Gupta, V.; DiPersio, J. F.; Catalano, J. V.; Deininger, M.; Miller, C.; Silver, R. T.; Talpaz, M.; Winton, E. F.; Harvey, J. H., Jr.; Arcasoy, M. O.; Hexner, E.; Lyons, R. M.; Paquette, R.; Raza, A.; Vaddi, K.; Erickson-Viitanen, S.; Koumenis, I. L.; Sun, W.; Sandor, V.; Kantarjian, H. M. *N. Engl. J. Med.* **2012**, *366*, 799.
- Thompson, J. E.; Cubbon, R. M.; Cummings, R. T.; Wicker, L. S.; Frankshun, R.; Cunningham, B. R.; Cameron, P. M.; Meinke, P. T.; Liverton, N.; Weng, Y.; DeMartino, J. A. *Bioorg. Med. Chem. Lett.* **2002**, *12*, 1219.
- Hexner, E. O.; Serdikoff, C.; Jan, M.; Swider, C. R.; Robinson, C.; Yang, S.; Angeles, T.; Emerson, S. G.; Carroll, M.; Ruggeri, B.; Dobrzanski, P. *Blood* **2008**, *111*, 5663.
- Manshour, T.; Quintas-Cardama, A.; Nussenzweig, R. H.; Gaikwad, A.; Estrov, Z.; Prchal, J.; Cortes, J. E.; Kantarjian, H. M.; Verstovsek, S. *Cancer Sci.* **2008**, *99*, 1265.
- Pissot-Soldermann, C.; Gerspacher, M.; Furet, P.; Gaul, C.; Holzer, P.; McCarthy, C.; Radimerski, T.; Regnier, C. H.; Baffert, F.; Drueckes, P.; Tavares, G. A.; Vangrevelinghe, E.; Blasco, F.; Ottaviani, G.; Ossola, F.; Scesa, J.; Reetz, J. *Bioorg. Med. Chem. Lett.* **2010**, *20*, 2609.
- Verstovsek, S. *Clin. Cancer Res.* **1988**, *2010*, 16.
- Ioannidis, S.; Lamb, M. L.; Wang, T.; Almeida, L.; Block, M. H.; Davies, A. M.; Peng, B.; Su, M.; Zhang, H.-J.; Hoffmann, E.; Rivard, C.; Green, I.; Howard, T.; Pollard, H.; Read, J.; Alimzhanov, M.; Bebernitz, G.; Bell, K.; Ye, M.; Huszar, D.; Zinda, M. J. *Med. Chem.* **2011**, *54*, 262.
- William, A. D.; Lee, A. C.-H.; Blanchard, S.; Poulsen, A.; Teo, E. L.; Nagaraj, H.; Tan, E.; Chen, D.; Williams, M.; Sun, E. T.; Goh, K. C.; Ong, W. C.; Goh, S. K.; Hart, S.; Jayaraman, R.; Pasha, M. K.; Ethirajulu, K.; Wood, J. M.; Dymock, B. W. *J. Med. Chem.* **2011**, *54*, 4638.
- Lim, J.; Taoka, B.; Otte, R. D.; Spencer, K.; Dinsmore, C. J.; Altman, M. D.; Chan, G.; Rosenstein, C.; Sharma, S.; Su, H.-P.; Szewczak, A. A.; Xu, L.; Yin, H.; Zugay-Murphy, J.; Marshall, C. G.; Young, J. R. *J. Med. Chem.* **2011**, *54*, 7334.
- Miyaura, N.; Suzuki, A. *Chem. Rev.* **1995**, *95*, 2457.
- Paquette, R. P.; Sokol, L.; Shah, N. P.; Silver, R. T.; List, A. F.; Clary, D. O.; Bui, L. A.; Talpaz, M. *Abstract of Papers*, 50th ASH Annual Meeting and Exposition, San Francisco, CA, 2008; Abstract 2810.
- Detailed experimentals and assay protocols for this manuscript are found in the following patent application: Mann, G.; Naing, A.; Arlyn, A.; Brown, S. D.; Chan, W. K. V.; Jeff, C.; Du, H.; Epshteyn, S.; Forsyth, T.; Galan, A. A.; Huyuh, T. P.; Ibrahim, M. A.; Johnson, H. W. B.; Brian, K.; Kearney, P.; Kim, B. G.; Koltun, E.; Leahy, J. W.; Lee, M. S.; Lewis, G. L.; Meyr, L. E.; Noguchi, R. T.; Pack, M.; Ridgway, B. H.; Shi, X.; Woolfrey, J.; Zhou, P. WO 2007/089768, **2007**.
- Mouse PK data*: **10d** was administered at 10 mg/kg PO or IV as a solution in water to female athymic nude mice ($n = 3$). *Rat PK data*: **10d** was administered at 5 mg/kg PO or IV as a solution in 5% EtOH 45% PEG400/Water + HCl to female CD Rats ($n = 3$). *Dog and cyno PK data*: **10d** was administered at 3 mg/kg PO or IV as a solution in 5% EtOH 45% PEG400/Water + HCl to either male beagle dogs or male cynos ($n = 3$).
- Shah, N. P.; Olszynski, L. S.; Verstovsek, S.; Hoffman, R.; List, A. F.; Cortes-Franco, J.; Kantarjian, H. M.; Gillman, D. G.; Clary, D. O.; Bui, L. A.; Wadleigh, M. *Abstract of Papers*, 50th ASH Annual Meeting and Exposition, San Francisco, CA, 2008; Abstract 98.